

УДК 615.47(045)

Nada Shokeh, Master Degree Student, Damascus University, Syrian Arab Republic  
Mhd. Aiman Al Akkad, Dr. Eng., Damascus University, Syrian Arab Republic

## FETUS ULTRASOUND 3D IMAGE CONSTRUCTION

Using 2D ultrasound devices doesn't offer clear images which leads to an imprecise diagnosis of the fetus state and doesn't reveal the fetus abnormalities. This led to the need for a 3D vision of the fetus by taking 2D visual sections of the fetus and assembling them to get a 3D model, in order to support medical agencies and private clinics with a computer system to produce and display 3D images of the fetus without the need to change their old equipment, the thing that give a powerful and inexpensive method to help gynecologist of making precise diagnostic decisions.

The methods of ultrasound scanning, 3D model construction and its visualization are presented. For data input the freehand scanning without a position sensor followed by segmentation and preprocessing procedures were used. For 3D construction the linear interpolation was used and the arbitrary plane slicing was applied for visualization.

Finally, some experiments were made using our automated system, and the results showed that the proposed method is simple, inexpensive and flexible, in comparison with available solutions.

**Key words:** free-hand scanning, position sensor, interpolation, ultrasound, 3D reconstruction, fetus.

The care of the fetus and his mother starts as early as possible where the growth of fetus is observed and the necessary tests are made to reveal illnesses and distortions where it became even possible to treat the fetus inside his mother.

Building a 3D model of the fetus, using available 2D ultrasound images to get a stereoscopic representation of the fetus, enables obstetrician and gynecologist from following the fetus growth and diagnoses his health state precisely and quickly.

Motivation for 3D ultrasound [1] is related to *volume measurements*. The acquisition of an entire volume allows the clinician to view desired 2D ultrasound images, which is otherwise not possible with conventional 2D systems due to the physical constraints of the scanning process, like a C-scan view, i.e. a 2D slice parallel to the skin surface. In 2D ultrasound systems, 3D images could only be imagined by the clinician by building up a mental picture from 2D information. But if a comprehensive 3D ultrasound data set is available then radiologist could navigate through the 3D volume to find the most diagnostically significant 2D slices. The reliability of the diagnosis would be further enhanced by the ability to capture multiple 2D views of the region of interest and thereby providing a means of validation. This could save cost of re-acquiring images and avoid inconvenience in case the radiologist is not satisfied with the 2D ultrasound image views. 3D Images are frequently easier to interpret especially for users not experienced in viewing cross-sectional 2D B-mode images. 3D Images may be more informative to physicians who become more confident with their interpretation of a 3D view than with a set of 2D cross-sections. The above issues strongly suggest the need for an easy-to-use, practical and low-cost quantitative 3D ultrasound acquisition method. 3D ultrasound offers the potential for improving the quality of a conventional 2D image, by compounding images acquired from different perspectives.

3D ultrasound differs from other medical imaging modalities in its irregular sampling of space, anatomy's appearance depends on the direction of insonification, and low signal to noise ratio of the images them-

selves. These differences affect the way the data is subsequently analyzed, e.g. visualization algorithms need to cope with the irregular spatial distribution of the B-scans, segmentation algorithms must be effective in the presence of speckle, shape fitting algorithms may need to interpolate through non-parallel contours, and registration algorithms must differentiate between real image discrepancies and those related to the direction of insonification.

3D reconstruction and elastography enable visualizing the fetal face, including clefts and abnormal facial features. It also helps in diagnosis of congenital abnormalities of a fetus and other birth defects, such as spina bifida or cleft palate. In cardiac examination, it can detect abnormalities not otherwise visible.

### Acquisition

There are essentially two ways to acquire 3D ultrasound data: using a *dedicated 3D probe*, which scans a small fixed volume area, or using a *freehand system* [17], in which the position and orientation of a *conventional 2D probe* are recorded as the probe is swept manually over the region of interest, and a 3D volume is constructed from the resulting B-scans and their relative positions.

Freehand 3D ultrasound is a technique for acquiring ultrasonic data of a 3D volume by recording the trajectory of the ultrasound 2D probe using a position sensor. Probe calibration is necessary to find the rigid body transformation from the coordinate system of the B-scan to that of the mobile part of the position sensor. In [2] a thorough analysis of acquisition approaches was introduced based on their accuracy, ease of use, reliability, and speed of calibration. Tracking a position sensor attached to a conventional ultrasound probe in a freehand 3D ultrasound system, allows a large volume to be recorded and visualized in a fixed global coordinate system. Different ultrasound imaging modes do exist:

– *A-mode (A for amplitude)*: The echo amplitude is displayed as a function of propagation length in one propagation direction, and is only used for precise distance measurements inside the ocular globe.

– *B-mode (B for brightness)*: B-mode image is produced by sweeping a narrow ultrasound beam through the region of interest while transmitting pulses and detecting echoes along a series of closely spaced scan lines.

– *M-mode (M for motion)*: A single beam in an ultrasound scan can be used to produce an M-mode picture, where movement of a structure such as a heart valve or tissue such as the myocardium can be displayed in a wave-like manner.

The resolution of an ultrasonic imaging system depends on several factors:

– *Axial*: It is in the direction of beam propagation. Axial resolution is the minimum separation between two interfaces located in a direction parallel to the beam so that they can be imaged as two different interfaces.

– *Lateral*: It is the other principal direction in the plane of B-scan. It is determined by focusing properties of the transducer. The lateral resolution is improved where the beam is focused dynamically by electronic or mechanical means.

– *Elevational*: This direction is perpendicular to the plane of B-Scan.

To improve the resolution, higher frequencies can be used, but it results in shorter maximal penetration depth. To compensate for the attenuation of ultrasound waves propagating through the tissue, the detected RF analog signal is amplified as a function of propagation time (thus propagation length), this is called *Time Gain Compensation (TGC)*, and is sampled at a high rate. The echo signal is retrieved by the demodulator by demodulation techniques called *quadrature demodulation*, where the samples contain both magnitude and phase information. The sampled signal is then logarithmically compressed to reduce the dynamic range from the sampled range and to nonlinearly map the dynamic range to enhance the darker-gray levels at the expense of the brighter gray levels [4].

While most commercial systems employ volume probes for good reasons of ergonomics and practicality, the freehand protocol allows the acquisition of arbitrarily sized volumes and consequently has more potential applications.

Freehand 3D ultrasound can be acquired without a position sensor by deducing the elevational probe motion from the inter-frame decorrelation, i.e. by exploiting *speckle decorrelation* [14, 15, 16] to determine out of plane transducer motion. However, a freehand scan involves lateral and axial, as well as elevational, probe motion, where lateral sampling is relatively sparse, and lateral motion tracking requires sub-sample interpolation.

### 3D reconstruction

The volume of the anatomy can be constructed by matching the ultrasonic data with its corresponding position in space. The mobile part of the position sensor records the 3D location of the sensor, rather than the scan plane, relative to its stationary counterpart, it is therefore necessary to find the position and orientation of the scan plane with respect to the electrical centre of the position sensor. This rigid-body transformation comprises six parameters: 3 translations in the direction of the  $x$ ,  $y$  and

$z$  axes and 3 rotations, azimuth, elevation and roll, about these axes. This transformation is determined through a process called *probe calibration* [3]. The stationary part of the position sensor is often called the *world coordinate system*, and the term position sensor is used to mean its mobile counterpart. Another issue before the construction of a volume in space is to determine the B-scans scales.

Several techniques have been described recently in the literature for the reconstruction of a regular volume out of a series of ultrasound slices with arbitrary orientations, typically scanned by means of ultrasound freehand systems. However, a systematic approach to such a problem is still missing. A *statistical* method for the construction and trimming of the sampling grid was carried out. Region of interest is smaller than those obtained from other reconstruction methods in those cases where the scanning trajectory deviates from a pure straight line. In addition, an adaptive *Gaussian interpolation* technique is studied and compared with well-known interpolation methods that have been applied to the reconstruction problem in the past. In 3D ultrasound the spatial relationships among 2D slices are preserved in the 3D volume, allowing an *off-line examination* of scans previously recorded even by another clinician.

3D ultrasound techniques can be classified as those derived from a 2D phased-array probe, and those that obtain a 3D data set from 2D B-scans acquired in rapid succession while the probe is in motion. The former technique employs a 2D array of piezoelectric elements and the volume is scanned by electronically steering the array elements. The main drawback of this technique is the limited field of view of the existing probes. The latter technique makes use of conventional 2D ultrasound systems and a positioning system. This technique includes both the freehand and the mechanically swept volume acquisition techniques. Each B-scan pixel, which is initially measured in the coordinate system of the probe, can be spatially located with respect to the fixed coordinate system by means of a vector of position and a vector of orientation that jointly comprise the six degrees of freedom between two 3D coordinate systems.

A simple *affine transformation* allows us to convert each position in the image plane to a position in 3D space. Calibration of the freehand system on which the accuracy of the overall system depends, is necessary and deals with finding the transformation between the image plane and the receiver coordinate system, providing an accurate registration of ultrasound images to 3D space [5, 6]. The acquired data can be seen as a scattered distribution of planes in 3D space due to the total freedom of the physician to perform the scanning procedure. Although a real-time visualization based on raw B-scans (without prior reconstruction) is possible and allows online diagnosis [7], and despite the existence of efforts of authors [8,9,10] to do signal processing directly on the raw data, a *regular grid* is still needed to apply further processing with available algorithms.

Ultrasound volume reconstruction tackled by several studies [11, 12, 13, 14] focused on incremental interpolation of the gaps between the slices, as well as on the de-

termination of the final intensity of a voxel when several B-scans overlap on this voxel (i.e. compounding). Specifically, [11] focuses on spatial compounding with image-based registration. The regular grid is filled using a nearest neighbor approach and compounding is simply an average operation, and the registration of B-scans is related to a baseline built from a quick pass over the region-of-interest. The registration step is intended to avoid blurring of miss-registered structures due to spatial compounding. An inverse distance weighting scheme explained in [10] follows, where each pixel that falls within a circular area of a fixed radius (centered at the voxel) contributes to the voxel value inversely to the distance from the voxel to the pixel.

A survey of well-known reconstruction methods like *voxel nearest neighbor*, *pixel nearest neighbor*, and *distance weighting* interpolation, were introduced in [13] in addition to a new interpolation method based on *radial basis function*. Finally, [14] apply a weighted *ellipsoid Gaussian convolution kernel* to tackle the reconstruction of irregularly-sampled data. All the above-mentioned studies, despite their unobjectionable quality, paid no attention to the details of the construction of the regular grid. However, this problem is of paramount importance for further data processing and storage.

*Nearest neighbor* interpolation, often produces discontinuous voxel reconstructions with prominent artifacts. Other interpolation techniques, such as *trilinear*, *B-spline* and *radial basis function interpolation*, consider not just the nearest pixel but also other nearby pixels, thereby arriving at *smoother reconstructions* at the expense of *computational speed*. 3D ultrasound is perhaps the only medical imaging modality for which a nearest neighbor interpolation is acceptable, since resolved structures in ultrasound images are fairly large compared with the intra-B-scan and inter-B-scan pixel spacing. Consequently, interpolation artifacts are relatively small in scale compared with the much larger structures of interest. Extensive quantitative and qualitative studies have shown that the improvement offered by radial basis function interpolation over nearest neighbor interpolation is marginal [18].

Before applying any interpolation (compounding) technique, the volume where the data are going to be re-sampled must be defined. The definition of the *volume grid* implies the selection of an *orientation* and *extent* for the volume and the selection of a *voxel size*. The reconstructed volume is preferred to resemble either the original sweep or some anatomical predefined plane. But, the problem of ultrasound imaging is that a standard scanning policy does not exist. Clinicians look for the best viewing direction (insonation angles) at will for each pregnant woman, attempting to avoid annoying effects like shadowing. Therefore, the overall scan may consist of several sub-scans from which a single scanning direction (principal direction) may not be clearly defined. This problem comprises three sub-problems: selection of the coordinate system of the reconstruction grid, selection of the extent of the reconstructed volume, and determination of the voxel size.

Principal component analysis (PCA) has been used to deal with the first of the aforementioned subproblems. Considering the 3D positions of the pixels as samples of a population, we look for the coordinate system that achieves the largest data variance in each direction while being uncorrelated with the others. The size of the reconstructed volume is pruned using the eigenvalues information provided by PCA. Furthermore, an adaptive Gaussian convolution kernel for dealing with irregularly sampled data is introduced and compared with some well known reconstruction techniques.

### Visualization

3D ultrasound can be visualized using techniques common to other medical imaging modalities, including *any-plane reslicing*, *multiplanar reformatting*, *non-planar reslicing*, *volume rendering* and *surface rendering* (following segmentation). More specific to 3D ultrasound is the way these displays are created from the raw data, which does not generally lie on a regular grid. To take advantage of the mature visualization packages already available, many 3D ultrasound systems start by resampling the raw data onto a regular grid, then employ existing techniques to visualize this grid. However, resampling inevitably involves interpolation and approximation, which can lead to artifacts in the resulting visualizations.

Slices that cannot be acquired because of the geometrical constraints imposed by other structures of the pregnant woman can now be readily rendered by the so-called *any-plane slicing*, where volume visualization and accurate volume estimation may greatly enhance the diagnosis task. A nearest neighbor algorithm for generating a reslice image directly from a set of B-scans and their relative positions can be used.

When resampling this data onto the regular grid, the intensity of the shaded voxel is decided by using nearest neighbor interpolation, where we search for the nearest B-scan pixel and set the voxel intensity accordingly. If we discount the convenience of available voxel visualization packages, we can question the wisdom of reconstructing a regular voxel array at all. If we wish to generate a reslice of the voxel array, we would once again use some sort of interpolation to set the intensities of the pixels which constitute the reslice image. We thus have 2 stages of interpolation: from the B-scans to the voxel array, and then from the voxel array to the reslice.

Each stage introduces errors, and it is reasonable to suppose that more faithful visualization is achievable by interpolating directly from the B-scans to the reslice. *Direct interpolation* has other advantages: visualization can proceed immediately after (even during) acquisition, with no delay while the voxel array is reconstructed, and there is no need for extra memory in which to store the voxel array. The one disadvantage is speed: the regularity of the voxel array makes it easy to generate reslices and volume renderings extremely quickly. In comparison, generating the same renderings directly from the B-scans is slower. While this is used to be a strong argument in favor of voxel arrays, the rapid increase in processor speeds has now tipped the balance the other way:

with perhaps the one exception of volume rendering, it is now possible to visualize the raw data at perfectly acceptable interactive rates, without the need for an intermediate voxel representation. To interpolate up to a maximum distance  $d$ , so that if any point in the reslice plane is further than  $d$  from a B-scan pixel, we leave it blank instead of shading it with misleading data. This is impractical when there is motion caused by the cardiac pulse, in which case we need to arrange instead for some form of gating, visualizing only those B-scans which belong to the same phase of the cardiac cycle. Data requires the prior segmentation to separate the structure of interest from the background.

Unfortunately, even manual segmentation of ultrasound images is difficult, given the low signal to noise ratio and the ubiquitous imaging artifacts. Speckle could be considered noise by an automatic segmentation algorithm, though it is readily suppressed by median filtering [19]. A more debilitating artifact is the disappearance of tissue boundaries when they lie parallel to the direction of insonification. For these reasons, generic 3D ultrasound segmentation techniques always rely on the skill of an expert operator, who either delineates the segmentation contours entirely manually, or in an attempt to speed up the process guides a semiautomatic algorithm, e.g. live-wire [20]. Subsequent processing of the contours, for volume measurement or shape analysis, can take the load off the operator by accepting as sparse a set of contours as possible, using a process of fitting a surface through a sparse contour set using a variant of shape-based interpolation [21]. Normally, the operator's expertise is replaced by a model of the structure to be segmented, allowing the segmentation algorithm to make informed decisions in regions of the image where the signal to noise ratio is poor. The danger of relying on *anatomical models* in this way is that, in describing where the segmentation boundary is most likely to be, they do not account for possible local pathology, which is often precisely what the segmentation is supposed to detect. High contrast boundaries are also sometimes apparent in obstetrics applications, where parts of the fetal surface may be clearly visible against the amniotic fluid.

As with other imaging modalities, we might wish to register two 3D ultrasound volumes to highlight changes over time, so it is important to use a flexible *similarity criterion* like the *correlation ratio* [22] or *mutual information* [24, 25], and not a simple sum of *squared difference* grey-level comparison. Registration algorithms used still a matter of active research, tend to reflect the mainstream in medical image registration, namely *spline deformations* to describe nonrigid registrations, multi-resolution searches for the optimal solution, and powerful similarity criteria, such as mutual information and the correlation ratio, to compare the two volumes. First the individual B-scans which make up a freehand 3D data set are registered, and limited to the underlying physical process. Thus, B-scan  $n+1$  is translated within its plane until it most closely matches B-scan  $n$ . Given that B-scans  $n$  and  $n+1$  were acquired almost simultaneously and therefore appear very similar, a simple similarity criterion like the sum of squared grey-level differences

will suffice. Following the translation, a non-rigid warp is applied in the axial direction to compensate for varying probe contact pressure. B-scans which have been compressed by the probe are retrospectively expanded to match the B-scan acquired with the minimum probe pressure, and to recapture how the anatomy would have appeared if scanned with a non-contact acquisition protocol [26].

The inter-B-scan registration process partially estimates the relative positions of B-scans without the need for a position sensor. It can be extended to encompass the out-of-plane displacement between pairs of B-scans, by exploiting the phenomenon of speckle regression [27] or *speckle decorrelation* [28], where the correlation between corresponding patches of speckle diminishes the further apart the patches are. By estimating the relative displacements of several patches of speckle at different points on neighboring B-scans, all six degrees of freedom of the B-scans relative location can be deduced, leading ultimately to a *position sensorless* freehand 3D ultrasound system. Another form of registration peculiar to 3D ultrasound is the alignment of partially overlapping sweeps for extended field of view imaging.

#### Experiments and results

In this research we are trying to introduce an effective and precise method to visualize the fetus in a realistic form based on available ultrasound images by taking many images from different positions and angles to send to a computer for manipulating and constructing the 3D model and giving a stereoscopic vision of the fetus allowing to see the width, height and depth and gender, and revealing fetus abnormalities. This is possible in the middle of the pregnancy but more clear in advanced pregnancy age. We hold our experiments in two main stages: *acquisition and preprocessing*, then *3D construction and visualization*.

First we define the region of fetus existence inside the pregnant woman's womb, and then regularly took B-scan sections of the fetus starting from the head till the bottom of his feet. The scan will be in the fetus region, where we will divide this region taking in consideration the size of the region and size of the probe with which we will practically make the scan, the probe we used is a convex probe with the following specifications: its width is 1.3 cm and its angle is  $86^\circ$  and its radius is 4.6 cm, and contains 256 crystals.

If the size of the region is less than 4.6 cm (the probe radius), we take as illustrated in figure 1a, 50 samples of each section starting from the head till the bottom of the feet while keeping sufficient acquisition precision then we take the average to compensate for fetus movement. We operated the ultrasonic device at 2 to 5.8 MHz and reached a depth of 16.5 cm. Slices sampling rate is 25 frames/sec.

But if the size of the region was greater than 4.6 cm, we divide as illustrated in figure 1b, the targeted region into two parts and we do in each part what we did in the previous procedure and for precision we adopt interleaving principle by taking sections in the middle between two section in order not to lose any important information. Now we've got many B-scan sections of the fetus

without missing any details. The optimal number of slices  $N_s$  should be the total sampling period  $T_t$  multiplied by the sampling frequency  $f_s$ :  $N_s = T_t \times f_s$ .

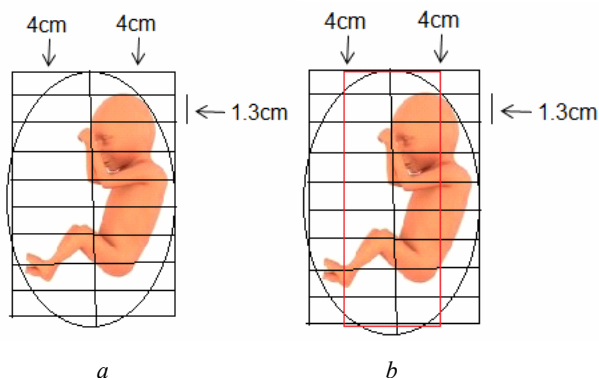


Figure 1. a – region division if its size < probe radius; b – region division if its size < probe radius.

3D reconstruction was made by filling the voxel grid based on the following calculations: slice (matrix) ele-

ment index with value “1” was divided by the number of matrix columns to get the voxel position where  $x$  is the result of division,  $y$  is the remain. The calculated depth  $z$  is the slice sequence number subtracted from the total number of slices, and the measured depth by the ultrasound device is referred to as  $z_m$ . Actually  $z$  should not exceed the length of the fetus, that’s why we have to multiply  $z$  by the ration  $l_c/l_m$ , where  $l_c$  is the fetus calculated length and  $l_m$  is the fetus measured length.

Instead of taking multiple sections manually, taking in consideration precision and the difficulty for the physician which may lead to losing information when the B-scan images are not precise, we found that making one sweep over the region (i. e. the physician keeps on a fixed speed and angle) taking a video clip of the fetus from the head till the bottom of the feet. Then we divide the video into multiple images (e. g. 300 images/video clip) which is difficult to achieve manually (the manual session takes 30 minutes while the video clip session takes 30 seconds). Figure 2 shows the user interface of our software.

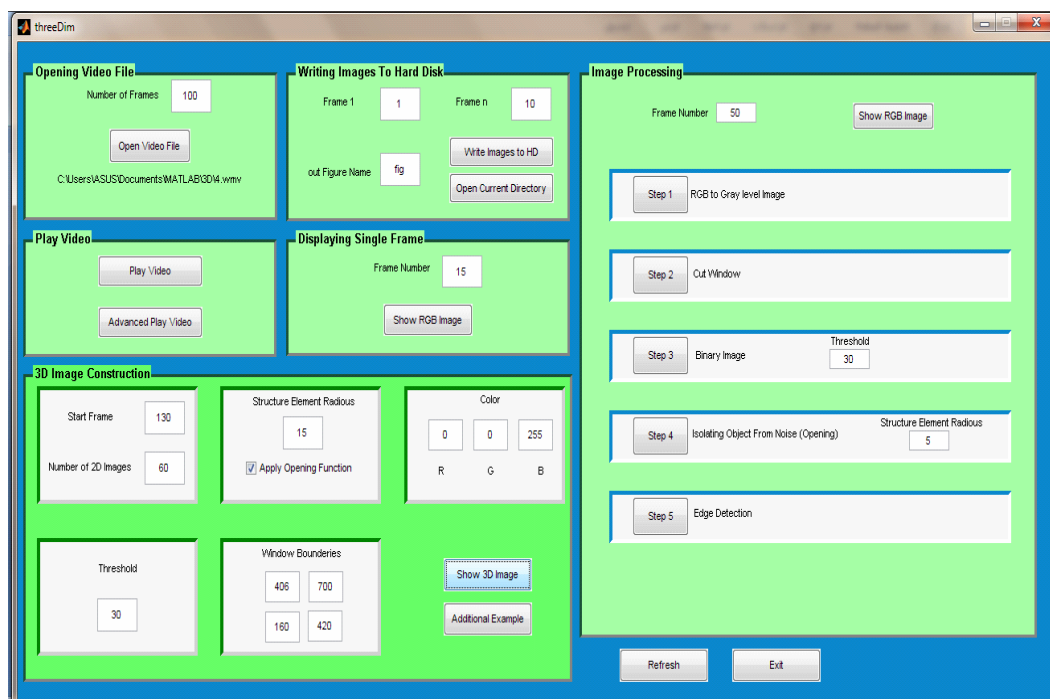


Figure 2. User interface of our software

In the acquisition stage we save B-scan images keeping their order then in the reconstruction stage we start building the volume matrix which consists of many voxels. The images we got contain a lot of unnecessary information and noise, so we process each image a part.

Suppose we have the image in figure 3a, and what we are interested in is only a certain part of it, as shown in figure 3b, so we cut this part then we use morphologic operations to treat noise, where the open transform in this case removes all the small elements by using a filtration window with a certain radius (we chose a value of 15 pixel), as shown in figure 3c, here decreasing the ra-

dius increases the details but also increases noise, and for transferring from grey level image to binary image we apply a conversion threshold (we chose a value of 20), which when decreased also details and noise increase, then we apply a segmentation filter (we used Sobel filter to define the B-scan segments contours as shown in figure 3d where the result is a zero element 2D matrix except contours are of value one, and we apply this for all images. At this point we apply linear interpolation by filling the voxel matrix by a sequence of B-scan images where the distance we should take between sections is the region length divided by the number of slices.

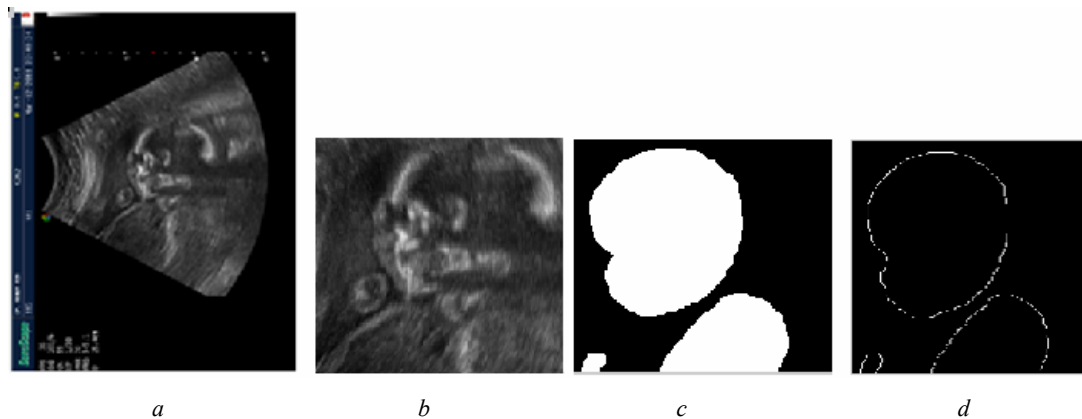


Figure 3. *a* – original ultrasound section; *b* – area of interest; *c* – binary image; *d* – object contours\

Decreasing the number of slices increases the speed of getting the 3D model of the fetus where the distance between sections is relatively large, but precision will decrease so we have here a trade off between precision and speed which can be initially defined experimentally.

We visualized the resulting voxel matrix by surface rendering using a skin color for the fetus deduced from the probability of his parents skin color. Filling the voxel matrix is shown in figure 4.

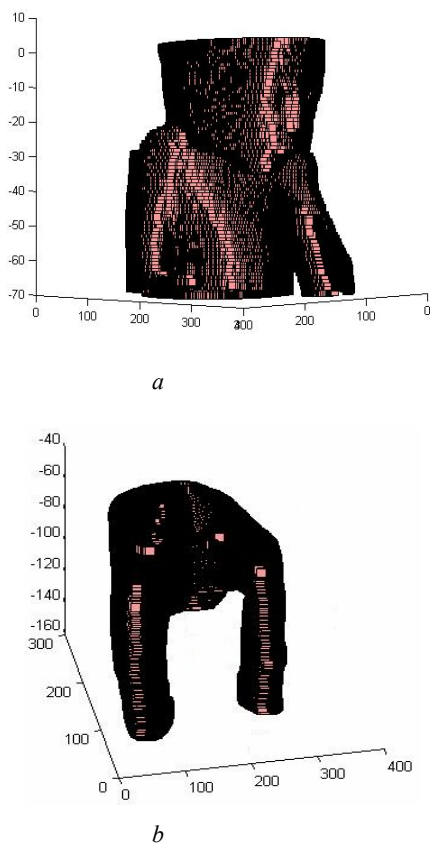


Figure 4. *a* – 3D model of the fetus upper part; *b* – 3D model of the fetus lower part

### Conclusion

We offered in this paper a system for 3D model construction of the fetus by resampling the raw data onto a regular grid and employed existing techniques to visu-

alize this grid, without the need to additional tools for the physician. What is only needed an ordinary 2D echo apparatus, a PC, and our dedicated software system. Our scheme displays in the final pregnancy weeks a full model of the fetus, while others display only part of the fetus.

Our approach's advantage over other available ones is its *low cost*, *flexibility* and *ease of use* for the physician while it doesn't need great experience, just a manual scan for a defined region of the pregnant woman belly, and another advantage is that it is *simple* and doesn't need a position sensor or a sophisticated processing as in speckle decorrelation method.

Preserving the spatial relationships among 2D slices in the resulting 3D volume allows an *off-line examination* of previously recorded scans even by another clinician, by taking advantage of the image processing and visualization packages already available, which forms a basic advantage.

### References

1. Freehand 3D Ultrasound Calibration: A Review / P. W. Hsu [et al.] // CUED/F-INFENG/TR 584, December 2007.
2. Engineering a freehand 3D ultrasound system / A. H. Gee [et al.] // Pattern Recognition Letters. 2003. – 24:757–777.
3. A review of calibration techniques for freehand 3D ultrasound systems / L. Mercier [et al.] // Ultrasound in Medicine & Biology. – 2005. – 31(4):449–471.
4. York G., Kim Y. Ultrasound processing and computing: Review and future direction // Rev. Biomed. Eng. – 1999. – 01:559-588.
5. 3D ultrasonic image feature location based on magnetic scan head tracking: In vitro calibration and validation / PR Detmer [et al.] // Ultrasound Med Biol. – 1994. – 20:923–936.
6. Prager R. W., Gee A., Berman L. Stradx: Real-time acquisition and visualization of freehand three-dimensional ultrasound // Med Image Anal. – 1999. – 3(2):129–140.
7. Treece G. M., Prager R. W., Gee A. H. Regularized marching tetra-hedra: Improved iso-surface extraction // Computer Graphics. – 1999. – 23(4): 583–598.
8. Surface interpolation from sparse cross sections using region correspondence / G. M. Treece [et al.] // IEEE Trans Med Imaging. – 2000. – 19(11):1106–1114.
9. 3D ultrasound measurement of large organ volume / G. M. Treece [et al.] // Med Image Anal. – 2001. – 5(2):41–54.

10. 3D freehand ultrasound: Image reconstruction and volume analysis / C. D. Barry [et al.] // *Ultrasound Med Biol.* – 1997. – 23(8):1209–1224.
11. Rohling R. N., Gee A. H., Berman L. 3D spatial compounding of ultrasound images // *Med Image Anal.* – 1997. – 1(3):177–193.
12. Sanches J. M., Marques J. S. A Rayleigh reconstruction / interpolation algorithm for 3D ultrasound // *Pattern Recogn. Lett.* – 2000. – 21(10):917–926.
13. Rohling R. N., Gee A. H., Berman L. A comparison of freehand 3D ultrasound reconstruction techniques // *Med Image Anal.* – 1999. – 3(4):339–359.
14. Meairs S., Beyer J., Hennerici M. Reconstruction and visualization of irregularly sampled 3D and 4D ultrasound data for cerebrovascular applications // *Ultrasound Med Biol.* – 2000. – 26(2): 263–272.
15. Speckle reduction imaging / D. Becker [et al.] // *GE Medical Systems, Ultrasound.* – 2003.
16. Speckle classification for sensorless freehand 3d ultrasound / G. M. Treece [et al.]. – University of Cambridge, 2005.
17. Optimally discriminant moments for speckle detection in real b-scan images / R. Marti [et al.] // *Ultrasonics, In Press.* – 2008.
18. Engineering a freehand 3D ultrasound system / A. H. Gee [et al.] // *Pattern Recognition Letters.* – 2003. – 24:757–777.
19. Rohling R. N., Gee A. H., Berman L. A comparison of freehand 3D ultrasound reconstruction techniques // *Med Image Anal.* – 1999. – 3:339–59.
20. Davies E. R. On the noise suppression and image enhancement characteristics of the median, truncated median and mode filters // *Pattern Recognition Letters.* – 1988. – 7:87–97.
21. Barrett W. A., Mortensen E. N. Interactive live-wire boundary extraction // *Med Image Anal.* – 1997. – 1:331–41.
22. Surface interpolation from sparse cross-sections using region correspondence / G. M. Treece [et al.] // *IEEE Trans Med Imaging.* – 2000. – 19:1106–14.
23. The correlation ratio as a new similarity measure for multimodal image registration / A. Roche [et al.] // *Medical Image Computing and Computer-Assisted Intervention, Cambridge MA, LNCS 1496, Springer, 1115–2, 1998.*
24. Multimodality image registration by maximization of mutual information / F. Maes [et al.] // *IEEE Trans Med Imaging.* – 1997. – 16: 187–98.
25. Viola P., Wells W. M. Alignment by maximization of mutual information // *Intr. Computer Vision.* – 1997. – 24:137–54.
26. Correction of probe pressure artifacts in freehand 3D ultrasound / G. M. Treece [et al.] // *Med Image Anal.* – 2002. – 6:199–215.
27. Sensorless freehand 3D ultrasound using regression of the echo intensity / R. Prager [et al.] // *Ultrasound Med Biol.* – 2003. – 29:437–46.
28. Automated 3D US frame positioning computed from elevational speckle decorrelation / T. A. Tuthill [et al.] // *Radiology.* – 1998. – 209:575–82.

---

Нада Шокех, магистрант, Дамасский университет, Сирийская Арабская Республика

Мхд. Айман Аль Аккад, кандидат технических наук, Дамасский университет, Сирийская Арабская Республика

### Построение 3-мерного ультразвукового изображения плода

2-мерные ультразвуковые устройства не позволяют получать четкие изображения, что ведет к неточной диагностике состояния плода и не позволяет обнаружить аномалии. Отсюда возникает потребность в получении 3-мерного изображения плода путем сборки 2-мерных изображений в 3-мерную модель. Это позволит медицинским учреждениям и частным клиникам, оснащенным вычислительными системами, создавать и отображать на экране 3-мерные изображения плода без необходимости замены прежнего оборудования. Это мощный и недорогой метод, который поможет гинекологам принимать правильные диагностические решения.

В данной статье описываются методы ультразвукового сканирования, построения и визуализации 3-мерной модели. Для ввода данных использовалась ручная сканер, затем выполнялась сегментация и предварительная обработка данных. Для построения 3-мерного изображения использовалась линейная интерполяция, а для визуализации – слайсинг (slicing) в произвольной плоскости.

С помощью автоматизированной системы были проведены эксперименты и получены результаты, подтверждающие простоту, дешевизну и гибкость предлагаемого метода по сравнению с существующими решениями.

**Ключевые слова:** ручной, позиционный датчик, интерполяция, ультразвук, восстановление 3-мерного изображения, плод.